Ab initio study of the electronic and structural properties of $CsSnI_3$ perovskite

Jean-François Chabot, Michel Côté, Jean-François Brière [a]

[a] Département de physique et Groupe de recherche en physique et technologie des couches minces (GCM), Université de Montréal, C. P. 6128 Succursale Centre-ville, Montréal (Québec) H3C 3J7, Canada,
email: michel.cote@umontreal.ca

The $CsSnI_3$ crystal belongs to an interesting class of semiconducting perovskite which is currently used in thin-film field-effect transistor made of organics-inorganics hybrid compounds. The benefit of using hybrid compounds resides in their ability to combine the advantage of these two classes of compounds: the high mobility of inorganic materials and the ease of processing of organic materials. In spite of the growing attention of this new material, very little is known about the electronic and structural properties of the inorganic part of this compounds. The $CsSnI_3$ is known to adopt 3 crystalline phases depending on the temperature: cubic (α-phase, $T_\alpha > 426K$), tetragonal (β-phase, $351K < T_\beta \leq 426K$) and orthorhombic (γ-phase, $T_\gamma \leq 351K$). We have calculated the electronic properties for these 3 phases within the frame work of density functional theory where a generalized gradient approximation was used to represent the exchange and correlation energy of the electrons. The calculations of the band structures show an increase of the band gap as the symmetry of the structure is reduced from the α to γ phases. All the calculations were carry out using the Abinit code and details of these calculations will be presented.

Le cristal de $CsSnI_3$ appartient à une classe intéressante de pérovskites semiconducteurs présentement utilisée dans les transistors à effet de champ basés sur des couches minces de composés hybrides organiques-inorganiques. L'avantage de ces composés hybrides tient à ce qu'ils combinent les qualités de ces deux classes de composés : la forte mobilité des inorganiques et la simplicité du procédé associée aux organiques. En dépit de l'attention croissante que l'on porte à ces matériaux, très peu de choses sont connues quant à la structure électronique de la partie inorganique. On sait que le $CsSnI_3$ adopte trois structures cristallines selon la température : cubique (phase α, $T_\alpha > 426K$), tétragonale (phase β, $351K < T_\beta \leq 426K$) et orthorhombique (phase γ, $T_\gamma \leq 351K$). Nous avons calculé la structure électronique pour ces trois phases dans le cadre de la théorie de la fonctionnelle de densité, où une approximation du gradient généralisée a été utilisée pour tenir compte des termes d'échange et de corrélation. Les calculs montrent une augmentation de la bande interdite quand la symétrie de la structure est réduite de la phase α à la phase γ. Tous les calculs ont été effectués avec le code Abinit *et les détails en sont présentés.*

1 Introduction

The family of perovskite crystals (ABX_3) is an interesting class of material which exhibit a vast range of physical properties (superconductivity, magnetoresistance, ferroelectric, ...)[1]. A new application for the perovskite is found in hybrid organics-inorganics material which was recently used in thin-film field-effect transistors [2] [3]. This hybrid compound is made of a layered perovskite which is attached by organic molecules on each side as showed in figure 1. This hybrid compound has the potential to combine the high mobility of inorganic crystal and the ease of processing of the organic compound. However, as reported by Kagan *et al.* [2], the measured mobility of the hybrid compound $(C_6H_5C_2H_4NH_3)_2SnI_4$ was found to be 0.6 $cm^2V^{-1}s^{-1}$ which should be compared with the 3D hybrid cubic perovskite $CH_3NH_3SnI_3$ mobility of 50 $cm^2V^{-1}s^{-1}$, i.e. the layered structure has a mobility 100 times lower. As a first step in order to understand the low mobility in the layered hybrid compound, we will study the electronic and structural properties of perovskite $CsSnI_3$. We choose $CsSnI_3$ instead of $CH_3NH_3SnI_4$ for the following reasons:

- Both belong to the same class of semiconducting perovskite halides [4]. This mean that their electronic and structural behaviors should be quite similar.
- The role of the cation Cs^{+1} and $(CH_3NH_3)^{+1}$ is essentially in donating their electron to the system.
- The Cs has only one valence electron compared to 15 for the CH_3NH_3.
- Only one atom need to be treated for the Cs instead of 3 different atoms for the CH_3NH_3. Furthermore, the molecule CH_3NH_3 decreases the symmetry of the crystal which would complicate the interpretation of our calculations.

In doing so, we will make the *ab initio* calculations much faster and simpler to analyse.

The perovskite structure ABX_3 (in our case A=Cs, B=Sn and X=I) is composed of two cations (A and B) and one anion (X). In the cubic structure the cation A is placed at the 8 corners of the cube and the cation B is placed at the center surrounded by 6 anions X at the face centers of the cube forming a regular octahedron around the cation B (see figure 2).

The purpose of this discussion will be to describe the *ab initio* calculations, to compare experimental and theoretical data, to compute and analyse the electronic band structures for the 3 structural phases of $CsSnI_3$, and to investigate the phase transition between the α and the β phases using the phonon band structure.

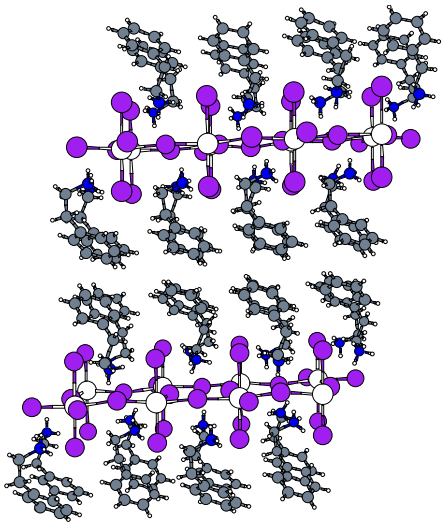

Figure 1. Organic-inorganic hybrid $(C_6H_5C_2H_4NH_3)_2SnI_4$ molecule

2 Computational Method

The results were obtained with the help of an *ab initio* method based on density functional theory (DFT) [5] [6] [7]. We use the Abinit code (www.abinit.org) [8] for all the calculations. Only the valence electrons are included explicitly and the effects of the core electrons are integrated in the pseudopotentials employed. The electronic wavefunctions are described by a plane wave basis set up to an energy cutoff of 30 Hartree and dense k-point grids were used to garanty convergence to better than 0.5 mHa/atom (for the α-phase: 8x8x8, β-phase: 6x6x6, and for γ-phase: 4x4x4, all shifted). Non-linear core correction was included for the alkaline atom. The exchange-correlation (xc) functional GGA (Generalized Gradient approximation) of Perdew-Burke-Ernzerhof was employed[9]. Response function calculations were also performed to get the phonon band structure.

The DFT is a method based on *ab initio* calculation initially proposed by Hohenberg, Kohn and Sham [10] [11] (1964-1965) which has the advantage to not rely on any experimental parameter. The idea of this method is to replace the interacting electronic system by a fictitious non-interacting electronic system which gives the same electronic density as the interacting system. The xc potential affecting the non-interacting electronic system can be obtained from the xc energy which is only a functional of the electronic density. However, no exact functional exists but many approximative functionals have been developed (LDA(local density approximation), GGA, ...).

The Kohn-Sham equations start in writing the Schrödinger's equation in the following form:

$$\left(-\frac{\hbar^2}{2m}\nabla^2 + V_{ion}(r) + V_H(r) + V_{xc}(r)\right)\Psi_j(r) = \varepsilon_j\Psi_j(r) \tag{1}$$

such that

$$n(r) = \sum_{j=occupied\ states} \Psi_j^*(r)\Psi_j(r). \tag{2}$$

Here $V_{ion}(r)$ is the ionic potential, $V_H(r)$ is the Hartree potential and $V_{xc}(r)$ is the xc potential obtained using some approximate functional. The last 2 potentials can be calculated knowing the density as shown in the following equations:

$$V_H(r) = e^2 \int \frac{n(r')}{\mid r - r' \mid} dr', \tag{3}$$

$$V_{xc}(r) = \frac{\delta E_{xc}[n(r)]}{\delta n(r)}, \tag{4}$$

where the form of $E_{xc}[n(r)]$ would depend on the chosen functional. For a given density $n(r)$ (call it the initial density $n_i(r)$), we first calculate V_H and V_{xc} and then find the eigenstates in solving the Schrödinger's equation (eq. 1). From the eigenstates $\Psi_j(r)$, the density $n(r)$ (call it the final density $n_f(r)$) is calculated using equation 2. Then, we pose $n_{i+1}(r) = n_f(r)$ and iterate the procedure until the initial and the final density converge to a common value, a procedure to assure self-consistency in the problem. This method gives in general results in excellent agreement with the experimental data such as lattice parameters, band structure, atomization energies, etc... However, the energy gaps from the band structures calculated with the DFT using the xc functional GGA or LDA are known to underestimate the experimental band gap but the result can be used to predict trends within a single family of compound.

3 Calculations

3.1 α, β and γ structures of the CsSnI3

The perovskite $CsSnI_3$ is known to exist in 3 different phases depending on the temperature [12]. At high temperature ($T > 426K$), the $CsSnI_3$ adopts a cubic structure (α-phase) as presented in the previous section (see figure 2). With decreasing temperature ($T < 426K$) the cubic structure change to a tetragonal structure (β-phase)(see figure 3). This structure is characterized by the rotation of the octahedra composed of iodine atoms about the center tin atom in a manner that each octahedron in the xy-plan rotates in opposite directions as we will show in subsection 3.3. Decreasing the temperature further ($T < 351K$), the tetragonal structure changes to an orthorhombic structure (γ-phase)(see figure 4). In this structure the rigidity of the octahedra is not conserved and the relative position of the cesiums atoms are distorted.

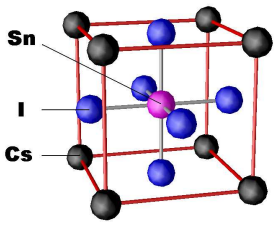

Figure 2. α-phase of the $CsSnI_3$

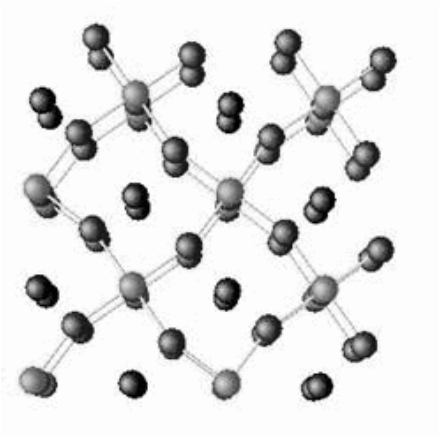

Figure 3. β-phase of the $CsSnI_3$

The figure 5 shows the calculations of the energies (Hartree / basic block of $CsSnI_3$) with respect to the volume for the 3 phases of the perovskite $CsSnI_3$. The γ-phase is represented by the lower curve, i.e. the curve with the smallest energies for a given volume. Since our calculations does not include any thermal motion of the atoms, corresponding essentially to a zero temperature limit, this result shows that the γ-phase is the most stable structure. The α-phase's curve (with the higher energies) and the β-phase's curve (with intermediate energies) represent structure which are stable for $T \neq 0$ where $T_\alpha > T_\beta$. This corresponds to the experimental observations from Yamada *et al.* [12].The volumes that minimize the energies of each phase are presented in table 1.

For the α-phase, all the atom positions are determined by the symmetry of the structure. The β and γ phases have a certain number of internal degrees of freedom which we can evaluate by a structural optimization for a given volume. The experimental atomic coordinations for these 2 phases are presented in table 2. For the β-phase, the c/a ratio is plotted in figure 6 and the internal parameters are plotted in figure 7. For the γ-phase, the c/a and a/b ratios are plotted in figure 8 and the internal parameters

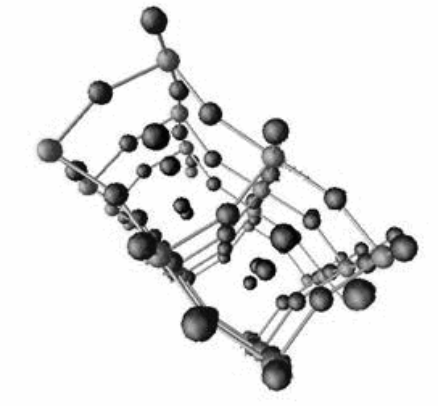

Figure 4. γ-phase of the $CsSnI_3$

Table 1
Experimental data [12] versus theoretical data of the lattice parameters and volume of the $CsSnI_3$ structures.

	lattice (exp.) (Å)	V_{exp} (Å^3/mol)	V_{th} (Å^3/mol)
α	a = 6.219	241	245 (+1.8%)
β	a = 8.772 c = 6.261	241	243 (+0.8%)
γ	a = 8.688 b = 8.643 c = 12.378	232	242 (+4.1%)

are plotted in figure 9. From these figures, the errors on the lattice parameters and the internal parameters are quite acceptable.

Table 2
Atomic coordinates of the β (with space group P4/mbm) and γ (Pnam) phases of the $CsSnI_3$.

	Atom	Position[1]	x	y	z
β	Cs	2d(mmm)	0	0.5	0
	Sn	2b(4/m)	0	0	0.5
	I(1)	2a(4/m)	0	0	0
	I(2)	4h(mm)	I_x	I_y	0.5
γ	Cs	4c(m)	Cs-x	Cs-y	0.25
	Sn	4b($\overline{1}$)	0.5	0	0
	I(1)	4c(m)	I(1)-x	I(1)-y	0.25
	I(2)	8d(1)	I(2)-x	I(2)-y	I(2)-z

From the curves of each phase we have performed the calculation of the bulk modulus ($B = -\frac{1}{V}\frac{\partial^2 E}{\partial V^2}$). The 3 bulk modulus are quite similar ($\sim$ 8 GPa) which was expected since the structures are nevertheless quite similar. No experimental data on the bulk modulus are available to

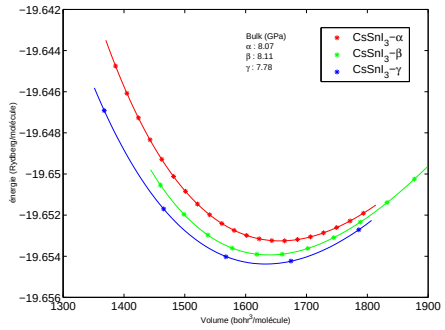

Figure 5. Energy vs Volume of the $CsSnI_3$ structures

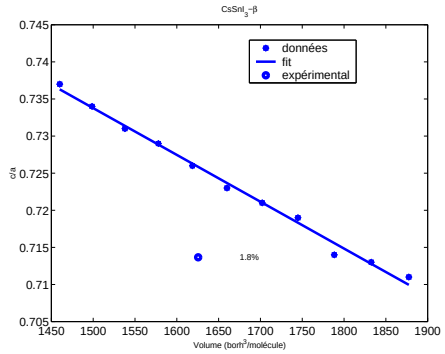

Figure 6. ratio c/a of the $CsSnI_3$-β

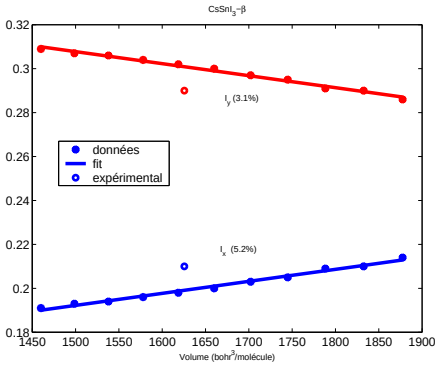

Figure 7. internal parameters of the $CsSnI_3$-β

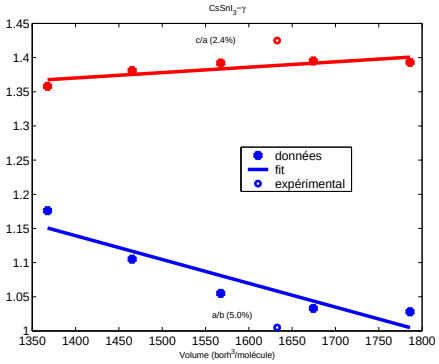

Figure 8. ratio a/b and c/a of the $CsSnI_3$-γ

make a comparison.

3.2 Band Structure

The band structure for the relaxed α-phase is shown in figure 10. The α-phase behaves like a semiconductor with a small gap ($E_{gap} = 0.434eV$) located at **R** ($\frac{1}{2}\frac{1}{2}\frac{1}{2}$) in the Brillouin zone. The conduction bands at that point are three fold degenerated whereas the valence band is a singlet. As we decrease the volume, the band gap decreases as showed in figure 14. For a certain volume the structure become metallic (see figure 11) and we observe, still at **R** point, that the last valence band joins with the two first conduction bands to form a triplet. The third conduction band now becomes a singlet. To explain this behavior, we have to know first that group theory of cubic system implies that the bands cannot be degenerated more than 3 times. This is why the triplet and the singlet cannot mix. For the semiconductor structure, when we look at the **R** $\rightarrow$ Γ direction, the symmetry group is smaller and the triplet split in a doublet and a singlet. Near the **R** point, the valence band singlet and the conduction band singlet have the same symmetry, and group theory postulate that such band cannot mix. Then, when we decrease the volume, the last valence and the first conduction band join each other, the two singlet repulse each other and the doublet becomes mixed with the singlet of the valence band showing a metallic form. The band structures for the relaxed structure of the β-phase and the γ-phase are showed in figure 12 and 13 respectively. We find a gap of 0.641 eV for the β-phase and 0.885 eV for the γ-phase. So we can observe that when we decrease the symmetry of the $CsSnI_3$, the gap becomes larger.

We have also calculated the gap of each structure with respect to the volume (figure 14). In general, for a given volume, the α-phase has the smallest gap and the γ-phase has the largest gap. The α-phase and the β-phase become metallic for a certain volume, which is not the case for the γ-phase.

3.3 Phonon band structure

The phonon band structure is shown in figure 15. Negative frequencies are used to represent imaginary frequencies. Such frequency are present at **M** ($\frac{1}{2}\frac{1}{2}0$) and **R** points and these correspond to instabilities in the α-phase as expected from the known phase transitions. We know that at T = 0K the β-phase and γ-phase are preferred to the α-phase, so we expect the α structure to be unstable. We have visualized the displacement vector at **M** and **R** points to distinguish which mode corresponds to the phase transi-

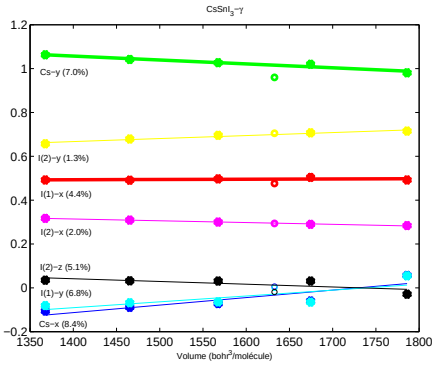

Figure 9. internal parameters of the $CsSnI_3$-γ

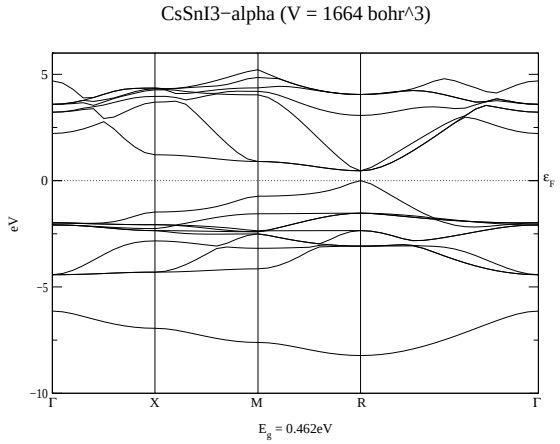

Figure 10. Bands structure of the $CsSnI_3$-α

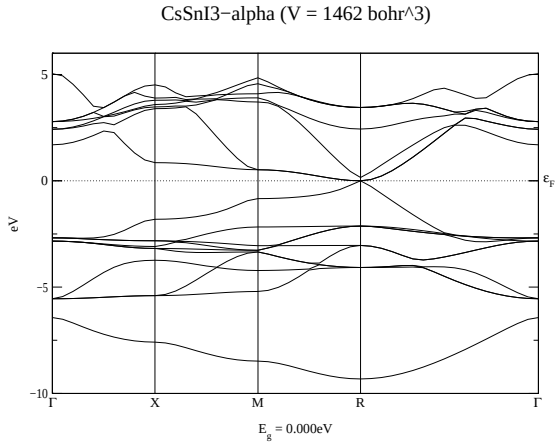

Figure 11. Bands structure of the $CsSnI_3$-α

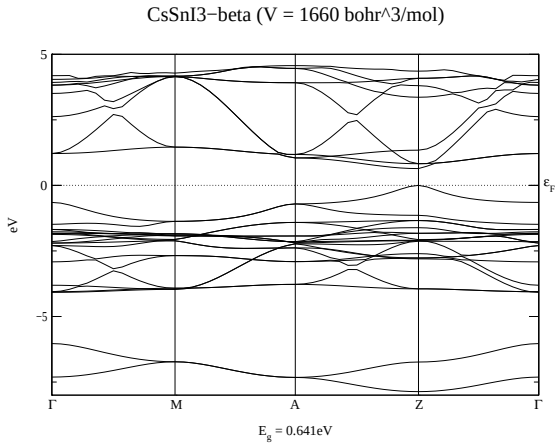

Figure 12. Bands structure of the $CsSnI_3$-β

tion to the β-phase.

In visualizing the displacement vector at M point we found that this corresponds to the transition to the β-phase. It looks like a rotation around the z-axis centered on the Sn atom which affects the iodine on the xy-plane. But for a given Sn, its nearest neighbors must rotate inversely because of the relative phase between the periodic cells given by the Bloch functions at **M** point. We can see this rotation in figure 16. Note that the β-phase preserve the rigidity of the octahedra formed by the iodines around the Sn atoms.

Now the visualization of the 3 displacement vectors at **R** point correspond exactly to the same vectors than at **M** point, but this time the rotation is about the 3 axes x, y and z. On a simple cubic first Brillouin Zone, there is 12 **M** points, but they are not all equivalent. There is 3 groups of 4 equivalent **M** points which each corresponds to rotation about one axis. Then the **R** point doesn't seem to correspond to the γ-phase transition because the γ structure can't be explained by using only the rotation about the Sn atom. Furthermore, the γ-phase doesn't respect the rigidity of the octahedra. The only way to explain the transition from the β-phase to the γ-phase is to plot the phonon band structure of the β structure and check the displacement vectors at the instable point.

4 Conclusion

We have showed in this article that the DFT calculations give good prediction on the lattice parameters of the $CsSnI_3$ and we can also predict the phase transition from the α-phase to the β-phase in computing the phonon band structure. The main purpose of this paper was to determine the electronic properties for the 3 structures of the $Cain_3$. We found that for high symmetric structure (α-phase) the band gap is smaller than the β-phase which is also smaller than the γ-phase.

Acknowledgments

This work has been supported by grants from the Natural Sciences and Engineering Research Council of Canada

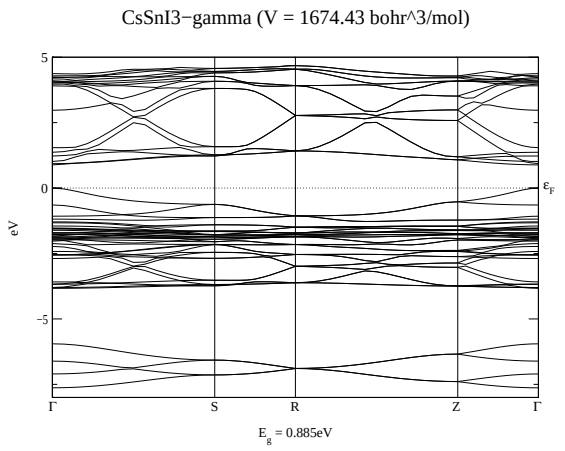

Figure 13. Bands structure of the $CsSnI_3$-γ

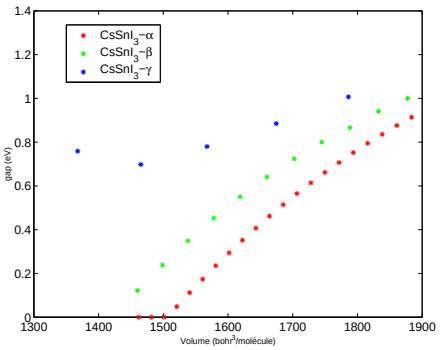

Figure 14. Bands structure of the $CsSnI_3$-γ

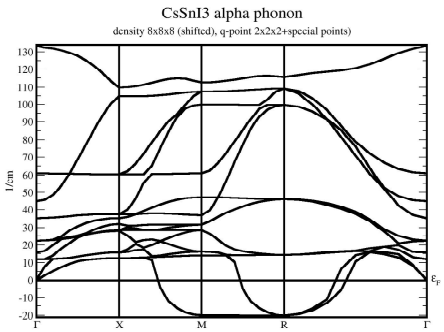

Figure 15. Phonon bands structure of the $CsSnI_3$-α

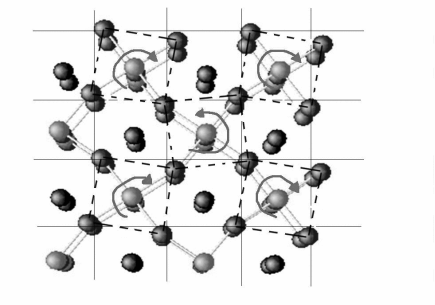

Figure 16. Rotation of the tin's atoms for the β-phase

(NSERC) and the Fonds québécois de la recherche sur la nature et les technologies (FQRNT). The computational resources were provided by the Réseau québécois de calcul de haute performance (RQCHP).

References

1. N. Mathur and P. Littlewood. Mesoscopic texture in manganites. *Physics Today, p.25*, January 2003.
2. C. R. Kagan, D. B. Mitzi, and C. D. Dimitrakopoulos. Organic-inorganic hybrid materials as semiconducting channels in thin-film field effect transistors. *Science, 286, 945*, 1999.
3. H. Klauk. Molecular electrics on the cheap. *Physics World, 13, 1, 18*, 2000.
4. D. B. Mitzi, C. A. Feild, Z. Schlesinger, and R.B. Laibowitz. Transport, optical, and magnetic properties of the conducting halide perovskite $ch_3nh_3sni_3$. *Journal of Solid State Chemistry, 114, 159*, 1995.
5. N. Argaman and G. Makov. Density functional theory: An introduction. *Am. J. Phys., Vol. 68, No. 1, p.69*, January 2000.
6. H. L. Neal. Density functional theory of one-dimensional two particles systems. *Am. J. Phys., Vol. 66, No. 6, p.512*, June 1998.
7. A. Schindlmayr. Universality of the hohenberg-kohn functional. *Am. J. Phys., Vol. 67, No. 10, p.933*, October 1999.
8. X. Gonze, J.-M. Beuken, R. Caracas, F. Detraux, M. Fuchs, G.-M. Rignanese, L. Sindic, M. Verstraete, G. Zerah, F. Jollet, M. Torrent, A. Roy, M. Mikami, Ph. Ghosez, J.-Y. Raty, and D.C. Allan. First-principles computation of material properties : the abinit software project. *Computational Materials Science 25, 478-492*, 2002.
9. Burke Perdew and Ernzerhof. Generalized gradient approximation made simple. *Phys. Rev. Lett. 77, 3865*, 1996.
10. P. Hohenberg and W. Kohn. Inhomogeneous electron gas. *Phys. Rev. 136, B864*, 1964.
11. W. Kohn and L. J. Sham. Structural phase transitions of the polymorphs of $cssni_3$ by means of rietveld analysis of the x-ray diffraction. *Phys. Rev. 140, A1133*, 1965.
12. K. Yamada, S. Funabiki, H. Horimoto, T. Matsui, T. Okuda, and S. Ichiba. Structural phase transitions of the polymorphs of $cssni_3$ by means of rietveld analysis of the x-ray diffraction. *Chemistry Letters, p.801*, 1991.